

An Advanced Modular Gravitational Reference Sensor for the Detection of Gravitational Waves in Space

SAPS BUCHMAN FOR THE STANFORD LISA COLLABORATION

Stanford University, Hanson Experimental Physics Laboratory, Stanford, CA 94305, USA

The Modular Gravitational Reference Sensor (MGRS) is based on the concept of a sensor independent of the rest of the experiment and is directly applicable to the Laser Interferometer Space Antenna (LISA) and its successor the Big Bang Observer (BBO). For interferometry the main laser beam will illuminate the MGRS housing, therefore separating the external interferometry from the housing-to-test-mass measurement. A double sided grating will further simplify the sensor structure and will improve the precision of the experiment. We present the recent progress at Stanford in developing the technologies required by the MGRS, including results in the areas of: a) an optical sensor design with measurement precision of $10 \text{ pm}/\sqrt{\text{Hz}}$, b) an angular sensor with measurement precision of $1 \text{ nrad}/\sqrt{\text{Hz}}$, c) numerical simulations of the optical measurements of the center of mass position of a spinning spherical proof mass indicating position precision of $3 \text{ pm}/\sqrt{\text{Hz}}$, d) the successful demonstration of the feasibility of fabricating localized grating patterns onto dielectric and gold materials, e) an advanced charge management system using an UV LED source, and f) measurements of surface patch effect potentials, a critical contributor to disturbance effects in accurate inertial sensors. We also discuss a LISA configuration with one spherical proof mass and in-field telescope pointing and present the advantages the MGRS and this architecture will bring to LISA and BBO.

1 The Modular Gravitational Reference Sensor

The Gravitational Reference Sensor (GRS), by physically shielding a proof mass from stochastic non-gravitational disturbances, provides the basis for following an inertial trajectory. By itself, or when integrated with a complete drag-free control system, the GRS opens new frontiers in Earth imaging and space science; autonomous maintenance and prediction of spacecraft orbits, satellite constellation maintenance without ground tracking, disturbance free inertial trajectories, new observations of the universe through gravity waves, new understanding of the physics of the Universe, precision formation flying for satellite constellation interferometers and imagers, geodesy and surface imaging, integrated precision inertial sensing of translation and rotation, autonomous spacecraft rendezvous, guidance and space-based target tracking.¹

A Disturbance Reduction System (DRS) is composed of the GRS, the actuating thrusters and the attitude and translation control algorithms. The first drag-free system, called DISCOS, was developed by Stanford University and launched on the U.S. Navy's TRIAD drag-free spacecraft in 1974.² Recently, GRS technology found application in space science, lying at the heart of the recently launched NASA Gravity Probe B mission to test Einstein's Theory of Relativity³. The GRS will again be crucial to the Laser Interferometer Space Antenna (LISA)⁴, part of the NASA SSE Strategic Plan; the LISA GRS will require disturbance reduction improvements of at least four orders of magnitude over current performance.

TRIAD I was launched September 2, 1972 with its Disturbance Compensation System (DIS-

COS) built by Stanford. Discos had 3 axis translation control and demonstrated an acceleration below $5 \times 10^{-11} \text{m/s}^2$ averaged over 3 days, corresponding to a residual acceleration of $2.7 \times 10^{-8} \text{m/s}^2/\sqrt{\text{Hz}}$ at $5 \mu\text{Hz}$.² GP-B was launched April 20, 2004 with drag-free control of all degrees of freedom, 3 translations and 3 rotations, and had a residual acceleration of $10^{-11} \text{m/s}^2\sqrt{\text{Hz}}$ at 13 mHz

The three main principles we applied in the design of a modern drag-free sensor are: a) Minimize the forces on the test mass (TM), b) Optimize the TM center of mass determination, and c) Use modern technology. In order to practically eliminate TM forcing we use a non-supported spinning spherical TM. The spin, at about 10 Hz, spectrally shifts the TM measurement noise, (including spin, precession, and polhode) above the science band; 1 Hz for LISA. A gap equal or larger than the TM diameter significantly reduces surface patch effect disturbances. A double sided grating on the sensor housing isolates the GRS from external measurements. The distance from the grating to the TM center of mass is measured directly, making the GRS modular, MGRS, and thus insulating it from other experimental systems.⁵ With the TM center of mass measured optically no active electrostatic systems are disturbing the TM. UV LEDs for charge control, gratings for non-transmissive optics advanced interferometry methods, and laser frequency doubling to green are some of the technologies that contribute to solving the challenges of advanced drag-free systems.

2 MGRS technologies

Optical sensing offers a high-resolution method of sensing across a large gap while maintaining low disturbances. The sensing element is a low-finesse Fabry-Perot 1.6 cm cavity formed between a Littrow mounted 900 lines/mm diffraction grating and the surface of the proof-mass. The sensor reached $10 \text{ pm}/\sqrt{\text{Hz}}$ sensitivity with $120 \mu\text{W}$ of optical power; figure 1a. Further improvements should achieve $1 \text{ pm}/\sqrt{\text{Hz}}$ sensitivity for $20 \mu\text{W}$ optical power in the LISA science band ($3 \times 10^{-5} \text{ Hz}$ to 1 Hz).

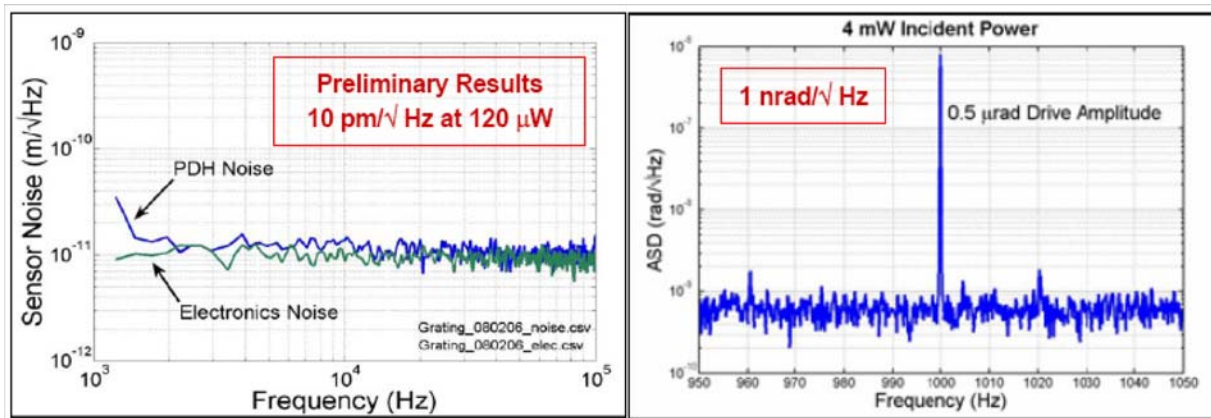


Figure 1: Performance of optical sensors: a) linear, b) angular

High precision angular sensing is needed in measuring the TM orientation, telescope steering, and point-ahead-angle control. We have demonstrated the use of grating diffraction orders as angular sensing signal beams, taking advantage of the grating angular magnification. The angular sensitivity achieved is better than $1 \text{ nrad}/\sqrt{\text{Hz}}$ with a 6 cm working distance; figure 1b.

A three dimensional numerical simulation of a sphere spinning at 10 Hz has been performed in order to demonstrate the feasibility of measuring the TM center of mass. Six optical sensors, with two sensors in the 60 degrees configuration of the LISA gratings are being used in the model. The position noise and surface roughness of the sphere are 50 nm. The results indicate that

the TM center of mass can be measured to $3 \text{ pm}/\sqrt{\text{Hz}}$. Further work incorporating additional disturbances is in progress: figure 2.

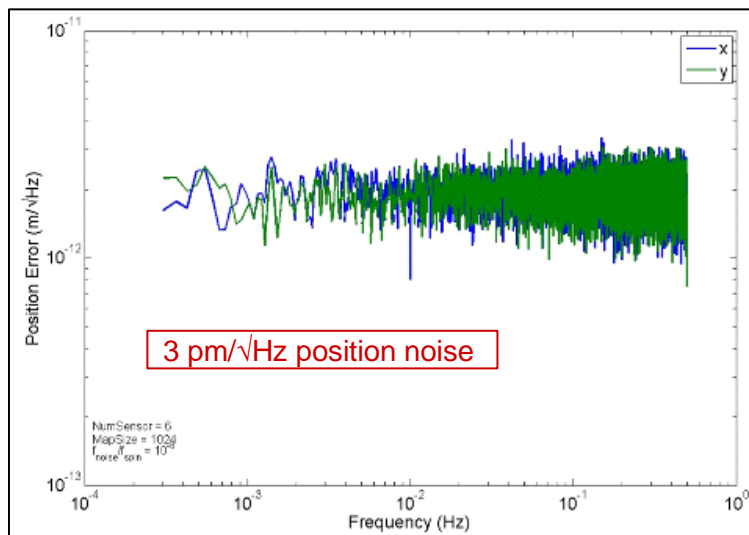


Figure 2: Numerical simulation of optical read-out of 10 Hz spinning sphere.

Since the tip/tilt sensor will require a grating atop the proof mass, we have demonstrated several ways of fabricating gratings on dielectric and gold surfaces: electron-beam lithography, mechanical transfer imprinting, and ion-beam writing. The grating patterns display only small irregularities caused mainly by the step size of the ion beam movement. Measured diffraction efficiencies meet requirements for the MGRS tip/tilt and displacement sensing.

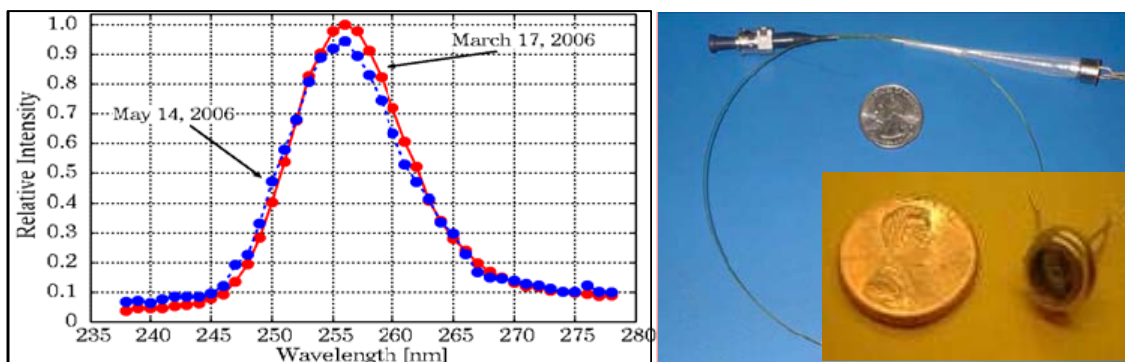


Figure 3: UV LED spectral stability, in TI05 packaging and coupled to optical fiber.

Charge management using photoelectrons has been demonstrated in the GP-B experiment using Hg discharge sources for the generation of the UV.⁶ Deep UV LED charge management systems have the advantages of high dynamic range, low disturbance, low power consumption, and light weight. We have demonstrated AC charge management using a UV LED, and have started the space qualification of these devices. A UV LED has operated for more than 8,000 hours under AC charge management working conditions. Additional measurements show power and spectral stability in the UV LED emission over this period of time. Figure 3 shows the UV LED spectral stability over 10 months and photographs of the LED in its TI05 packaging and coupled to an optical fiber.

A major noise source for the MGRS is due to spatial and temporal variations in surface potential (or patch effect) across the surfaces of the test mass and its housing. Such variations

will lead to force gradients which will result in a significant acceleration noise term. We have used a Kelvin probe to make spatial and temporal measurements of contact potential differences for a selection of materials (Au/Pt, beryllia, alumina, titanium) and coatings (gold, diamond-like carbon, indium tin oxide, titanium carbide). The data showed evidence of variations in the patch potentials related to pressure and contamination effects. Temporal variation measurements were limited by the current accuracy of the instrument.⁷ Figure 4 shows examples of Kelvin probe spatial scans and a photograph of the system.

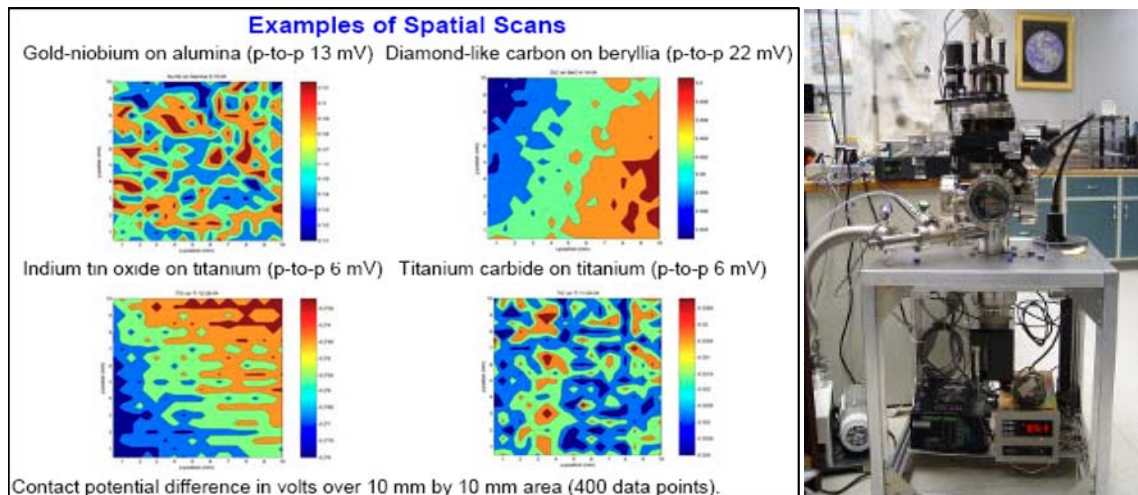


Figure 4: Kelvin probe: a) Spatial scans of coatings, b) Apparatus

3 Conclusions

The MGRS makes possible the achievement of drag-free performances appropriate for the future generation of space experiments. Among its design features are the complete elimination of electrostatic forcing and sensing, its isolation from other experimental systems, a spherical test mass spinning above the science measurement band, optical linear and angular sensing and gaps larger than the size of the sphere. Technologies that will ensure the performance and reliability of space-based gravitational wave detectors include the MGRS, in-field laser beam pointing, the use of gratings as non-transmissive optics, lasers with frequency doubled to green, and UV LED charge management.

References

1. D. B. DeBra, *Class. Quantum Grav.* **14** (6), 1549 (1997).
2. D. B. DeBra, *APL Technical Digest*; vol.12, no.2, p.14-26 (April-June 1973).
3. J. P. Turneaure, et al., *Advances in Space Research* (UK), vol **9**, 29-38 (1989).
4. K. Danzmann and A. Rudiger, *Class. Quantum Grav.* **20** (10), S1 (2003).
5. K. X. Sun, et al., *Class. Quantum Grav.* **22** (10), S287 (2005).
6. S. Buchman, et. al., *Review of Scientific Instruments* **66**, 120 (1995)
7. N. A. Robertson, et al., *Class. Quantum Grav.* **23** (7), 2665 (2006).